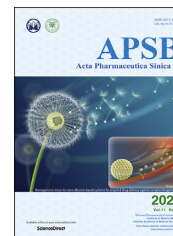




Chinese Pharmaceutical Association
Institute of Materia Medica, Chinese Academy of Medical Sciences

Acta Pharmaceutica Sinica B

www.elsevier.com/locate/apsb
www.sciencedirect.com



ORIGINAL ARTICLE

Salmonella flagella confer anti-tumor immunological effect *via* activating Flagellin/TLR5 signalling within tumor microenvironment



Jianxiang Chen^{a,c,e,†}, Yiting Qiao^{a,d,†}, Guo Chen^a, Cunjie Chang^c,
Heng Dong^c, Bo Tang^b, Xiawei Cheng^a, Xiufeng Liu^a,
Zichun Hua^{a,b,f,*}

^aSchool of Life Sciences, Nanjing University, Nanjing 210023, China

^bChangzhou High-Tech Research Institute of Nanjing University and Jiangsu TargetPharma Laboratories Inc., Changzhou 213164, China

^cCollege of Pharmacy, School of Medicine, Hangzhou Normal University, Hangzhou 311100, China

^dDivision of Hepatobiliary and Pancreatic Surgery, Department of Surgery, the First Affiliated Hospital, School of Medicine, Zhejiang University, Hangzhou 310003, China

^eDepartment of Hepatology, the Affiliated Hospital of Hangzhou Normal University, Hangzhou Normal University, Hangzhou 311121, China

^fSchool of Biopharmacy, China Pharmaceutical University, Nanjing 211198, China

Received 9 December 2020; received in revised form 2 April 2021; accepted 15 April 2021

KEY WORDS

Bacteria-mediated cancer therapy;

Abstract *Salmonella*: mediated cancer therapy has achieved remarkable anti-tumor effects in experimental animal models, but the detailed mechanism remains unsolved. In this report, the active involvement of the host immune response in this process was confirmed by comparing the tumor-suppressive

Abbreviations: AKT, Akt serine/threonine kinase; CFU, colony-forming units; CTLA-4, cytotoxic T-lymphocyte-associated protein 4; DN, dominant-negative; ERBB2, Erb-B2 receptor tyrosine kinase 2; ERK1, extracellular regulated protein kinase 1; GAPDH, glyceraldehyde-3-phosphate dehydrogenase; GFP, green fluorescent protein; i.p., intraperitoneally; i.t., intratumorally; IFN- γ , interferon- γ ; IL, interleukins; I κ B, inhibitor of NF- κ B; JNK, c-Jun N-terminal kinase; LPS, lipopolysaccharide; LRR, leucine-rich repeat; MyD88, myeloid differentiation factor 88; NF- κ B, nuclear factor kappa-B; PBS, phosphate-buffered saline; PCR, polymerase chain reaction; PD-1, programmed cell death protein-1; PD-L1, programmed cell death-ligand 1; PEI, polyethylenimine; TIR, Toll/Interleukin-1 receptor; TLR, Toll-like receptor; TME, tumor microenvironment; TRAF6, TNF receptor associated factor 6.

*Corresponding author.

E-mail address: zchua@nju.edu.cn (Zichun Hua).

[†]These authors made equal contributions to the work.

Peer review under responsibility of Chinese Pharmaceutical Association and Institute of Materia Medica, Chinese Academy of Medical Sciences.

<https://doi.org/10.1016/j.apsb.2021.04.019>

2211-3835 © 2021 Chinese Pharmaceutical Association and Institute of Materia Medica, Chinese Academy of Medical Sciences. Production and hosting by Elsevier B.V. This is an open access article under the CC BY-NC-ND license (<http://creativecommons.org/licenses/by-nc-nd/4.0/>).

Salmonella;
VNP20009;
Flagellum;
Flagellin;
TLR5;
NF- κ B;
Cancer immune therapy

effects of *Salmonella* in immunocompetent and immunodeficient mice bearing melanoma allografts. Since flagella are key inducers of the host immune response during bacterial infection, flagella were genetically disrupted to analyse their involvement in *Salmonella*-mediated cancer therapy. The results showed that flagellum-deficient strains failed to induce significant anti-tumor effects, even when more bacteria were administered to offset the difference in invasion efficiency. Flagella mainly activate immune cells via Flagellin/Toll-like receptor 5 (TLR5) signalling pathway. Indeed, we showed that exogenous activation of TLR5 signalling by recombinant Flagellin and exogenous expression of TLR5 both enhanced the therapeutic efficacy of flagellum-deficient *Salmonella* against melanoma. Our study highlighted the therapeutic value of the interaction between *Salmonella* and the host immune response through Flagellin/TLR5 signalling pathway during *Salmonella*-mediated cancer therapy, thereby suggesting the potential application of TLR5 agonists in the cancer immune therapy.

© 2021 Chinese Pharmaceutical Association and Institute of Materia Medica, Chinese Academy of Medical Sciences. Production and hosting by Elsevier B.V. This is an open access article under the CC BY-NC-ND license (<http://creativecommons.org/licenses/by-nc-nd/4.0/>).

1. Introduction

Bacteria were recognized as a potential cure for cancer a century ago¹. Many experimental therapies have been designed using *Salmonella*², *Bifidobacterium*³, *Escherichia*⁴, *Clostridium*⁵ and *Listeria*⁶, and these approaches have achieved remarkable anti-tumor effects in various animal models. Initially, the bacterial anti-tumor activity was attributed to the lysis of tumor cells after bacterial infection, especially for pathogenic *Salmonella*⁷. Later, increasing evidence indicated the involvement of the host immune response in the process of bacteria-mediated cancer therapy⁸.

Salmonella infection activates a cascade of immune responses. Upon entry of *Salmonella* into the body, neutrophils, inflammatory monocytes and natural killer cells are recruited to eliminate the bacteria, which is an innate immune response. Then matured macrophage and dendritic cells activate T-cells to initiate an adaptive immune response, marked by the expansion of *Salmonella*-specific T cell⁹. Both lipopolysaccharide (LPS) and Flagellin are important pathogen associated molecular patterns (PAMPs) that activate the host immune response. Flagellin is recognized by Toll-like receptor 5 (TLR5) on monocytes, macrophages, dendritic cells and CD4⁺ T cells¹⁰, while LPS can be recognized by multiple receptors, including TLR4 and CD14, on a wider range of leukocytes^{11,12}. Even though LPS is genetically deleted due to safety reasons, Flagellin/TLR5 recognition remains a crucial way for host immune activation by VNP20009.

Although weaker than *Salmonella*, tumors are also immunogenic, with various biomacromolecules released by necrotic tumor cells, creating a unique tumor microenvironment (TME) that induces the infiltration of inflammatory cells¹³. Natural killer cells and CD8⁺ T cells are able to destroy tumor cells mainly via necrosis mediated by secreted perforin and granzymes, as well as via induction of programmed cell death^{14,15}. Meanwhile, CD4⁺ T cells secrete interferon- γ (IFN- γ) and tumor necrosis factor- α (TNF- α) to suppress the tumor growth and induce cytolysis^{16,17}. Furthermore, IFN- γ and interleukins (ILs) secreted by CD4⁺ T cells can recruit a large number of macrophages, CD8⁺ T cells and B cells to the sites of tumors and active these cells¹⁶.

The density of intratumoral T cells is positively correlated with a good prognosis for many kinds of solid tumors, including melanoma¹⁸. However, a considerable percentage of the intratumoral T cells are dysfunctional due to the presence of regulatory T cells, M2-like macrophages and immunosuppressive cytokines, as well as the lack of costimulatory signals in the TME¹⁹. Moreover,

cancer cells often express ligands for immune checkpoint receptors to suppress the activation of T cells^{20,21}. Therefore, immunotherapies such as programmed cell death protein-1 (PD-1)/programmed cell death-Ligand 1 (PD-L1) antibodies, which aim to enhance the host immune response against malignant cells, have exhibited considerable clinical benefits in cancer patients²².

Anti-cancer bacteria could be an economical and targeted alternative for stimulating the intratumoral host immune response, since they are able to specifically colonize solid tumors and be rapidly eliminated by antibiotics after a treatment cycle¹. Various attenuated *Salmonella* strains have been developed for the study of *Salmonella*-mediated cancer therapies, among which VNP20009 has shown remarkable therapeutic effects in animal models and is the only strain to be evaluated in a phase I clinical trial^{23,24}. For unknown reasons, its anti-cancer efficacy was drastically weaker in human patients than in animal models²⁴. Therefore, a more thorough understanding of the mechanism by which *Salmonella* causes tumor regression is required for the rational design of potent yet safe therapies for human cancer patients.

In this study, the efficacy of VNP20009-mediated cancer therapy was compared in wild-type mice and nude mice to investigate the importance of T cell-mediated adaptive immune response for the anti-tumor activity of *Salmonella*. Then, genetically engineered strains of VNP20009, in which the key components of flagellum were deleted, were generated to analyse the involvement of Flagellin/TLR5/nuclear factor kappa-B (NF- κ B) pathway. Such flagellum-deficient strains exhibited a significantly impaired ability to suppress tumor growth due to poorer intratumoral colonization and the abrogation of the Flagellin/TLR5/NF- κ B pathway in the lymphocytes. Our findings suggest the possibility of improving the number and the activity of intratumoral T cells by stimulating the Flagellin/TLR5/NF- κ B pathway in the TME to boost the host immune response against tumor during *Salmonella*-mediated cancer therapy.

2. Materials and methods

2.1. Mice, cell lines and bacteria strains

6–8-week-old female C57BL/6 mice and BALB/c nude mice were purchased from Laboratory Animal Center of Yangzhou University, China. B16F10 mouse melanoma cells and Jurkat cells were purchased from American Type Culture Collection and maintained by methods described previously²⁵. Lipid A-modified

(*msbB*-), auxotrophic (*purI*-) *Salmonella typhimurium* VNP20009, *Escherichia coli* SM10 λ pir and TOP10 strains were obtained from American Type Culture Collection and were grown as manufacturer's instructions. All experiments involving mice were approved by Animal ethics committee of Nanjing University (Nanjing, China).

2.2. The construction of flagellum-deficient strains of VNP20009

Two flagellum-deficient strains deleting *flhD* or *fliE* were constructed by amplifying 5' flanking (primer DU1: TAGGAGCTCAAACAGCCTGTTTCGATCTGTTTC, DU2: GCGATGGAGTTGATAATCTTGGCGCTCG and EU1: CATGAGCTCCAGGTGATGATTIATTTAT, EU2: CTGCGTAAAAATCGCCAGGGCTGACAA) H1 and 3' flanking (primers DD1: ACTCCATCGCGACGCAACTCTACTCGTC, DD2: AGCAAGCTTTCATAACTCGCTCCTTGATTGC and ED1: GATTTTTACGCAGCAGATTACAGT, ED2: TAGTCTAGAGAATTTTCTGATCAAGCA) H2 DNA fragments. The amplified fragments were digested and cloned into pEX18Gm to generate the deletion plasmids pEX18Gm Δ *flhD* and pEX18Gm Δ *fliE*. The plasmids were introduced into *E. coli* SM10- λ pir for replication of these suicide plasmids and then electroporated into VNP20009 using MicroPulser Electroporator (Bio-Rad) by condition 1.6 kV, 25 μ F, 400 Ω . Single crossover deletion clones with the entire plasmids integrated into genome were selected on LB agar plates containing 50 μ g/mL gentamicin. Single colonies were carefully isolated from gentamicin plates using pipette tips, dissolved in 50 μ L LB broth and cultivated on 5% sucrose LB agar plates for 24–36 h at 28 °C to induce the resolution of inserted plasmids from bacteria genome. During the resolution (also called “double-crossover”), the targeted gene would be deleted through homologous recombination in a very small percentage of clones. Single colonies were picked from sucrose LB plates by pipette tips and dissolved in 20 μ L LB broth. 2 μ L of LB broth containing bacteria were used for polymerase chain reaction (PCR) verification. The *flhD* and *fliE* deletion strains were confirmed by PCR using typing primers TD1, TD2 and TE1, TE2. TD1: CCCAGGTCATAAAC CAGTCTGTGG, TD2: GACGTACCCCTATTCAGCAGTGTGG, TE1: TCTTGCCGCTGCCCGTTATTCA, TE2: CGTTTTGGCCCA CAGCACCAT.

2.3. Electron microscopy of bacteria

Overnight culture of VNP20009 was diluted 1:100 into fresh LB and grown to OD₆₀₀ ~0.8. Bacteria were collected and washed in 0.1 mol/L NaCl, and resuspended in phosphate-buffered saline (PBS). To examine cells by electron microscopy, 10 μ L of the culture was placed onto carbon-coated nickel grids (Electron Microscopy Sciences) for 1 min, washed 3 times with sterile water and then negatively stained with 0.2% uranyl acetate for 30 s. The samples were visualized using the JEM2100EX electron microscope (JEOL)²⁶.

2.4. Green fluorescent protein (GFP) gene transfection into VNP20009

VNP20009 and its flagellum-deficient strains were grown at 37 °C to mid-logarithmic phase in liquid LB and harvested at 4 °C. Bacteria (2.0×10^8) were dissolved in 40 μ L 10% glycerol and

then mixed with 1 μ L of peGFP (Clontech) vector for electroporation with the MicroPulser Electroporator (Bio-Rad) according to the manufacturer's instructions.

2.5. Bacteria adhesion and invasion assay

B16F10 melanoma cells were maintained and prepared for bacterial adherence and invasion assay as described before. The VNP20009 and the deletion strains were grown in liquid LB with constant shaking at 37 °C to reach OD₆₀₀ = 0.8–1.0, and then added to cell monolayers (2.0×10^5 cell/well) in 24-well plates at a ratio of 50:1 (bacterial cells:tumor cells) and inoculated for 1 h. The protocol of invasion and adhesion assay has been described previously²⁷.

In brief, for the adhesion assay, bacteria were added to the cell monolayer and incubated for 2 h. Non-adhered bacteria were washed away and the infected cells were lysed with sodium deoxycholate. Bacteria were serially diluted, spread onto modified LB agar plates (without sodium chloride) and incubated at 37 °C for 24 h before counting colony-forming units (CFU). For invasion assay, bacteria were added to the cell monolayer and incubated for 6 h. Extracellular bacteria were washed away and cleared by 1 h of treatment with 50 μ g/mL gentamicin. Then the cells were lysed with sodium deoxycholate and the CFU was determined as indicated above.

Also, the melanoma cells were infected by the bacteria carrying GFP as described above. Cells were fixed with 4% paraformaldehyde for 15 min at room temperature and rinsed with PBS for 3 times. Cell nucleus was stained with DAPI. The number of bacteria and melanoma cells were quantified by fluorescence microscopy. In brief, the cryosections of tumors were cut at 6 μ m thickness and fixed with methanol for 10 s. Cell nuclei were stained with DAPI, and the slides were visualized by the FV1000 confocal microscope (Olympus).

2.6. Evaluation of antitumor effects of VNP20009 and its flagellum-deficient strains

C57BL/6 mice or BALB/c nude mice were implanted subcutaneously with 5×10^5 B16F10 cells in 0.1 mL PBS on the mid-right side. Bacteria were prepared as previously described, and treated intraperitoneally (i.p.) or intratumorally (i.t.) at indicated doses of VNP20009. The antitumor activity of treatments was evaluated as previously described. The tumor volumes were determined using Eq. (1):

$$\text{Tumor volume} = \text{Length} \times \text{Width}^2 \times 0.52 \quad (1)$$

2.7. Evaluation of peripheral and intratumoral bacteria in vivo

To evaluate the efficacy of tumor colonization and the replication ability of different bacteria strains by different methods of treatment, mice bearing melanoma allografts were i.p. administered with 10^5 CFU/mouse or i.t. administered with 10^7 CFU/tumor of bacteria. Peripheral blood was drawn from eyeballs after 1, 2 and 3 h. Serially diluted blood was spread onto modified LB agar plates (without sodium chloride) and incubated at 37 °C for 24 h. The titre of bacteria (CFU/mL blood) was determined by counting colonies and dividing them by the volume of blood.

On Day 2 post-treatment, mice were sacrificed. Tumors were harvested aseptically homogenized with PBS at a ratio of 5:1 [PBS volume (mL):tumor weight (g)]. Serially diluted homogenates were spread onto modified LB agar plates (without sodium chloride) and incubated at 37 °C for 24 h. The titre of bacteria (CFU/g tissue) was determined by counting colonies and dividing them by the weight of the tissue.

2.8. Evaluation of intracellular bacteria number *in vivo*

To evaluate bacteria internalization *in vivo*, tumor masses were injected with 10⁸ VNP20009 or its flagellum-deficient strains (all strains carrying GPF plasmids) and then processed for confocal analysis and gentamicin protection assays.

Gentamicin protection assays were conducted on tumors resected 30 min after the administration of VNP20009, Δ *flhD* and Δ *fliE* strains. After resection, tumors were dissected, digested and smashed through 70 μ m cell strainers (Corning), and depleted of RBC by incubation with red blood cell lysis buffer on ice for 5 min. After that, the tumor cells were treated with 50 μ g/mL gentamicin for 2 h at 37 °C to eliminate the extracellular bacteria. Then the cells were counted and lysed with sodium deoxycholate to release the intracellular bacteria. The number of bacteria was measured by colony formation assay as described above.

2.9. Evaluation of antitumor effect of VNP20009 and Δ *fliE* strains with the same intracellular bacteria number

To check if the intracellular infection ability by different bacteria determined their antitumor effects, we tested different doses of VNP20009, Δ *flhD* or Δ *fliE* strains to ensure equivalent intracellular bacteria in tumor. As a result, 2 \times 10⁸ CFU of Δ *fliE* intratumoral treatment resulted in equivalent intracellular bacteria compared to 10⁵ CFU of VNP20009 intratumoral treatment on the next day post-treatment, but even to 10¹¹ CFU/tumor Δ *flhD* treatment still could not reach similar intracellular bacteria number as VNP20009 or Δ *fliE* treatment. The evaluation of antitumor effect under equivalent intracellular bacteria was conducted as described above.

2.10. Flow-cytometry analysis of splenocytes and intratumoral leukocytes

Mice bearing melanoma allografts were i.p. injected with PBS, VNP20009 and two flagellum-deficient strains. The tumors and spleens were resected after 6 days. Half of the tumor mass was dissected and incubated in PBS containing collagenase I (Gibco), collagenase IV (Sigma–Aldrich), DNase I (Sigma–Aldrich) and hyaluronidase (Worthington) for 1 h at 37 °C. Then the cell suspension was filtered through a 70 μ m cell strainer to form single cell suspension. Then red blood cells were removed by 5 min of incubation with red blood cell lysis buffer on ice. The mice spleens were smashed thoroughly between frosted glass slides and filtered through a 70 μ m cell strainer to prepare single cell suspension. Then red blood cells were removed by 5 min of incubation with red blood cell lysis buffer on ice.

After that, cells were stained with following antibodies: anti-CD4-PE (#553652, BD Pharmingen), anti-CD8-FITC (#561966, BD Pharmingen), anti-F4/80-PE (#565410, BD Pharmingen) and were processed for flow cytometry analysis by Cytomic FC 500MCL flow cytometer (Beckman Coulter).

2.11. The extraction of total RNA and RT-PCR

Total RNA was purified using a Trizol Plus kit (Invitrogen). First-strand cDNA synthesis was performed on 5 μ g of total RNA using the QuantiTect Reverse Transcription kit (Qiagen). Gene expression levels were determined by PCR analysis. The following primers are used: *Ii4*-Forward: CCATATCCACGGATGCGACA; *Ii4*-Reverse: AAGCCCGAAAGAGTCTCTGC; *Ii5*-Forward: CGTGGGGTACTGTGGAAAT; *Ii5*-Reverse: CTCAGCCTCAGCC TTCCATT; *Ii13*-Forward: CACACAAGACCAGACTCCCC; *Ii13*-Reverse: CTCATTAGAAGGGGCCGTGG; *Ii17a*-Forward: ACTACCTCAACCGTTCCACG; *Ii17a*-Reverse: GGACCAGGATCTCTTGCTGG; *Ii21*-Forward: GGAGACTCAGTTCTGG TGGC; *Ii21*-Reverse: TCTGTGGGAACGAGAGCCTA; *Ii22*-Forward: TGCGATCTCTGATGGCTGTC; *Ii22*-Reverse: CCTCGGAACAGTTTCTCCCC; *Iifng*-Forward: GCTACACACTG CATCTTGGC; *Iifng*-Reverse: GCATCCTTTTTTCGCCTTGCT; *Gapdh*-Forward: CCCTTAAGAGGGGATGCTGCC; *Gapdh*-Reverse: ACTGTGCCGTTGAATTTGCC.

2.12. Purification of T cells from tumors

Tumors were injected with PBS, VNP20009 and two flagellum-deficient strains, and were resected after 6 days. The tumor mass was dissected and incubated in PBS containing collagenase I (Gibco), collagenase IV (Sigma–Aldrich), DNase I (Sigma–Aldrich) and hyaluronidase (Worthington) for 1 h at 37 °C. Then the cell suspension was filtered through a 70 μ m cell strainer (Corning). Tumor-infiltrating T cells were enriched using CD3 Dynabeads (Thermo Fisher Scientific) according to manufacturer's instructions. In brief, 1 \times 10⁷ total tumor cells were suspended in 1 mL isolation buffer, and incubated with 25 μ L CD3 Dynabeads for 20 min at 4 °C. The tube was placed in a magnet for 2 min. Then the supernatant containing unwanted tumor cells were discarded. The magnetic beads were washed 3 times with cold PBS. The enriched CD3⁺ T cells were lysed for RNA extraction by adding cell extraction buffer of Trizol Plus kit (Invitrogen) to the magnetic beads.

2.13. Western blots and immunohistochemistry

Western blots were performed as depicted previously²⁸ and the following antibodies were used: NF- κ B P65 (sc-8008, Santa Cruz Biotechnology), phospho-P65 (#3039, Cell Signaling Technology), P38 (sc-398305, Santa Cruz Biotechnology), phospho-P38 (sc-166182, Santa Cruz Biotechnology), AKT serine/threonine kinases (AKT, sc-81434, Santa Cruz Biotechnology), extracellular regulated protein kinase 1 (ERK1, sc-271269, Santa Cruz Biotechnology), phospho-ERK1/2 (sc-81492, Santa Cruz Biotechnology), c-Jun N-terminal kinase (JNK, sc-7345, Santa Cruz Biotechnology), phospho-JNK (sc-6254, Santa Cruz Biotechnology), Flag (#F1804, Sigma–Aldrich), inhibitor of NF- κ B (I κ B, #9242, Cell Signaling Technology), glyceraldehyde-3-phosphate dehydrogenase (GAPDH, #2118, Cell Signaling Technology), and Flagellin (ab93713, abcam).

For immunohistochemistry, the resected tumor tissues were fixed with 4% formaldehyde, embedded in paraffin and sectioned. Immunohistochemistry staining was performed with CD45 antibody (ab10558, Abcam) according to standard histological procedures.

2.14. The construction of expression plasmids

Full length mouse *Tlr5* gene was cloned (primer TLR5-1: GATGGCATGTCAACTTGACTTGC; TLR5-2: TATGCGGCCG CCTAGGAAATGGTTGCTATGG) from B16F10 melanoma cell and ligated into modified pRK5-Flag vector (Addgene). The mouse dominant-negative (DN) plasmids were generated with pRK5-Flag vector by amplifying the sequence as following: myeloid differentiation factor 88 DN (*Myd88*-DN) (Δ 1-435, with primers MyD-1: ATTGGATCCGGCATCACCACCCTTGATGACC, MyD-2: TATCTCGAGTCAGGGCAGGGACAAAGCCTTGG), TNF receptor associated factor 6 DN (*Traf6*-DN) (Δ 1-864, with primers TRAF-1: ATTGGATCCGCCCTCTCATCCCGGGGAT, TRAF-2: CTCCTCGAGTCACTGGAAACCCTCTTCCGAA), *Tlr5* leucine-rich repeat domain DN (LRR-DN) (Δ 907-1707, with primers LRR-1: GATGGCATGTCAACTTGACTTGC; LRR-2: AAAACACG AAGCGAAGAGAAGATAAAGCCGTGCG; LRR-3: CGCACGGCTTATCTTCTCTTCGCTTCGTGTTTT; LRR-4: GCGAAGCTTTCAGGAAATGGTTGCTATGGTT) and *Tlr5* Toll/Interleukin-1 receptor domain DN (TIR-DN) (Δ 2041-2575, with primers TIR-1: GATGGCATGTCAACTTGACTTGC; TIR-2: TTAGCGGCCGCTCAGTCCCTGAACACCAGCTTC).

2.15. NF- κ B luciferase reporter assay

Jurkat cells were plated in 24-well plates with the density of 5×10^4 cells/well, and transfected with polyethylenimine (PEI, Yeasen) and expression plasmids at the ratio of 5 μ L PEI: 1 μ g plasmid. 0.5 μ g mouse NF- κ B-P65 firefly luciferase reporter plasmid was transfected with 0.1 μ g *Renilla* luciferase reporter vector as an internal control. After 24 h, cells were treated with 10 ng/mL recombinant Flagellin (Sigma–Aldrich) for 10 min to 4 h, and harvested for luciferase reporter assays with the Dual-Luciferase system (Promega) following the manufacturer's instructions. The NF- κ B promoter activity was quantified by calculating the ratio of *Firefly* luciferase signal and *Renilla* luciferase signal, and then the basal promoter activity level of the control group without the Flagellin treatment was adjusted to 1. The data were presented as the mean \pm standard deviation (SD) of triplicate experiments.

2.16. The intratumoral injection of lentivirus overexpressing TLR5 and its dominant-negative isoforms

Tlr5, *Tlr5*-LRR-DN and *Tlr5*-TIR-DN were subcloned from pRK5-Flag vector to pLenti-GIII-CMV-GFP-2A-Puro vector (Applied Biological Materials) using the following primers: Flag-5': AGACGAGCTAGCATGGACTACAAAGAC. TLR5-3': AGCAGTCTAGACTAGGAAATGGTTGCTATGG. LRR-3': AGCAGTCTAGATCAGGAAATGGTTGCTATGGTT. TIR-3': AGCAGTCTAGATCAGTCCCTGAACACCAGCTTC.

1×10^7 HEK293T cells were seeded in a 10 cm dish one day ahead and transfected with 4 μ g pLenti-GIII-CMV-GFP-2A-Puro expression vector and 4 μ g Third Generation Packaging Mix (Applied Biological Materials) by mixing with PEI at the ratio of 1 μ g plasmid:3 μ L PEI to produce lentivirus. The medium containing virus were collected at 48 and 72 h after the transfection, and passed through 0.45 μ m membranes to remove cell debris. Virus was concentrated by PEG8000-precipitation method and titrated as previously described²⁹.

C57BL/6 mice were inoculated with melanoma allografts as described above. When tumors could be detected, the mice were randomly grouped as 9 mice/group. On Days 7, 9 and 11 post inoculation, 2×10^6 U of lentivirus overexpressing TLR5 or DN proteins were injected into tumors with 20 μ L of DMEM. On Day 10, a low dose (1000 CFU/mouse) of VNP20009 was injected into tumors. On Day 16, mice in pTIR-DN and pTIR-DN + VNP20009 groups were randomly divided into two subgroups and injected with lentivirus expressing TLR5 or the empty vehicle at the same dosage as the first treatment. Then the anti-tumor effects were evaluated.

2.17. Bio-Plex Multiplex Suspension Array

Tumor tissue was weighed and homogenized for 1 h on ice in 50 mmol/L HEPES (pH 7.4), 100 mmol/L NaCl, 50 mmol/L NaF, 2 mmol/L EDTA, 1% Triton-100 and 100 μ g/mL phenylmethanesulfonylfluoride. Cytokines were measured using the Bio-Plex Suspension Array System (Bio-Rad) according to the manufacturer's protocols as described previously²⁵.

2.18. Statistical analysis

Unpaired Student's *t* test analysis was carried out on data using the SPSS software to assess statistical significance. Differences between experimental groups were considered significant when $P < 0.05$. * $P < 0.05$; ** $P < 0.01$; and *** $P < 0.001$.

3. Results

3.1. VNP20009 showed weakened anti-tumor activity in immunodeficient mice

To test whether the host immune response has a crucial role in VNP20009-mediated cancer therapy, subcutaneous melanoma allografts were established on both immunocompetent and immunodeficient mice using murine B16F10 cells. A single intraperitoneal administration of VNP20009 could achieve a 93.3% reduction in tumor volume in the immunocompetent mice, while the reduction rate fell to 48.9% in the immunodeficient mice (Fig. 1A–D). A similar trend was also observed following intratumoral treatment with VNP20009 (Supporting Information Fig. S1A–S1D). Additionally, strong immunohistochemical staining for CD45 in tumor tissues resected from VNP20009-inoculated immunocompetent mice indicated a high infiltration of inflammatory cells after *Salmonella* infection (Fig. 1E). In addition, the level of IL-2, mainly secreted by activated CD4⁺ T cells, was significantly increased in tumors resected from immunocompetent mice (Fig. S1E). These results suggest that the host immune response is an important factor influencing the anti-tumor activity of VNP20009.

3.2. Flagella deletion of VNP20009 reduced its anti-tumor activity in immunocompetent mice, but not in immunodeficient mice

VNP20009 carries a deletion of the *msbB* gene to reduce systemic toxicity associated with LPS²³. However, the structure of flagellum remains intact and is still able to activate monocytes, macrophages, dendritic cells and CD4⁺ T cells. Moreover, flagella are also the locomotory organelles of *Salmonella*. To test the

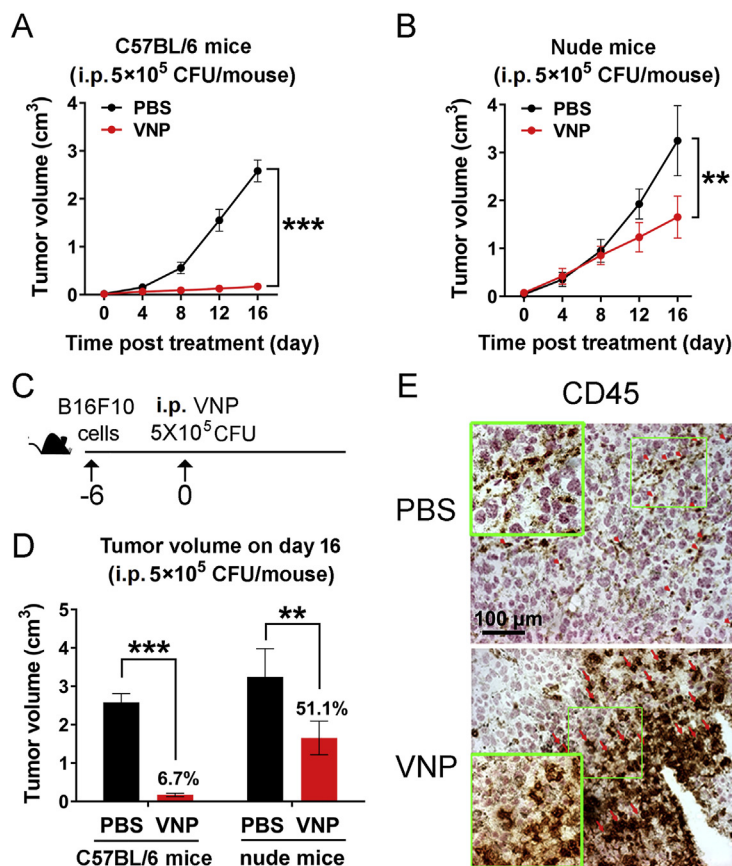


Figure 1 VNP20009 exhibited stronger anti-tumor activity in immunocompetent mice, compared with immunodeficient mice. Immunocompetent (A) and immunodeficient (B) mice carrying melanoma allografts were intraperitoneally administrated with phosphate-buffered saline (PBS) or VNP20009 (labelled as VNP in the figure). The tumor volumes were recorded and plotted as means \pm SD, $n = 8$ for immunocompetent mice, $n = 10$ for immunodeficient mice. (C) The treatment schedule for mice bearing B16F10 melanoma allografts. (D) The tumor volumes at the end of experiments (Day 16). Data are mean \pm SD, $n = 8$ for immunocompetent mice, $n = 10$ for immunodeficient mice. (E) The representative immunohistochemical staining of CD45⁺ cells of tumors resected from immunocompetent mice bearing melanoma allografts on Day 6 after VNP20009 treatment. Red arrow indicated CD45⁺ cells. Images in large green squares were the enlargement of images within small green squares. ** $P < 0.01$; *** $P < 0.001$; n.s. stands for nonsignificant. i.p. stands for intraperitoneally.

importance of flagella in VNP20009-mediated cancer therapy, the flagella deletion strains Δ *flhD* (one of the master regulatory genes in flagella organization) and Δ *fliE* (a basal body structure protein) were constructed by double-crossover gene replacement (Fig. 2A and B, and Supporting Information Fig. S2A)³⁰. Neither Δ *flhD* or Δ *fliE* strains expressed Flagellin, nor could they form flagella (Fig. 2C and Fig. S2B). In immunocompetent mice, the flagellum-deficient strains failed to reduce the volume of tumors (Fig. 2D) or extend the survival of mice (Fig. 2E), indicating that the anti-tumor activity was mostly lost in the flagellum-deficient strains. Δ *fliE* had a slightly better anti-tumor effect than Δ *flhD*. However, this remarkable difference in the anti-tumor activity between the wild-type VNP20009 and the flagellum-deficient strains was substantially diminished in immunodeficient mice (Fig. 2F and G).

These results indicate that flagella play a crucial role in VNP20009-mediated cancer therapy, partially in a host immune response dependent manner.

3.3. Weakening of infectivity partially explained the loss of anti-tumor activity of the flagellum-deficient strains

For the host immune system, flagellum are pattern recognition ligands, while they are also important locomotive organelles for

microorganisms. The destruction of flagella would affect the mobility and infectivity of VNP20009, having minimal effects on the bacterial growth (Fig. S2C). Δ *flhD* exhibited weakened adhesion to cell monolayers (Fig. 3A), and both Δ *flhD* and Δ *fliE* showed significantly impaired invasive tendency *in vitro*, with Δ *flhD* exhibiting almost complete loss of the invasive ability (Fig. 3B, Supporting Information Fig. S3A and S3B).

Fluorescent microscopy of tumor tissues infected with GFP-labelled VNP20009 showed that bacteria invaded tumors cells during *Salmonella*-mediated cancer therapy (Fig. 3C), suggesting that adhesion and invasion are two important steps for successful intratumoral colonization. Our results also showed that the destruction of flagella had a fundamental influence on bacterial behaviour during cancer therapy *in vivo*. First, the flagellum-deficient strains were cleared from the peripheral blood much more rapidly than the wild-type strain. By 2 h after intraperitoneal administration, most flagellum-deficient VNP20009 had been eliminated, while wild-type VNP20009 still persisted in the peripheral circulation (Fig. 3D).

Moreover, bacterial colonization in the tumors was also significantly poorer for the flagellum-deficient strains, especially when they were administered i.p. (Fig. 3E). Direct intratumoral injection narrowed the gap in the intracellular bacteria number

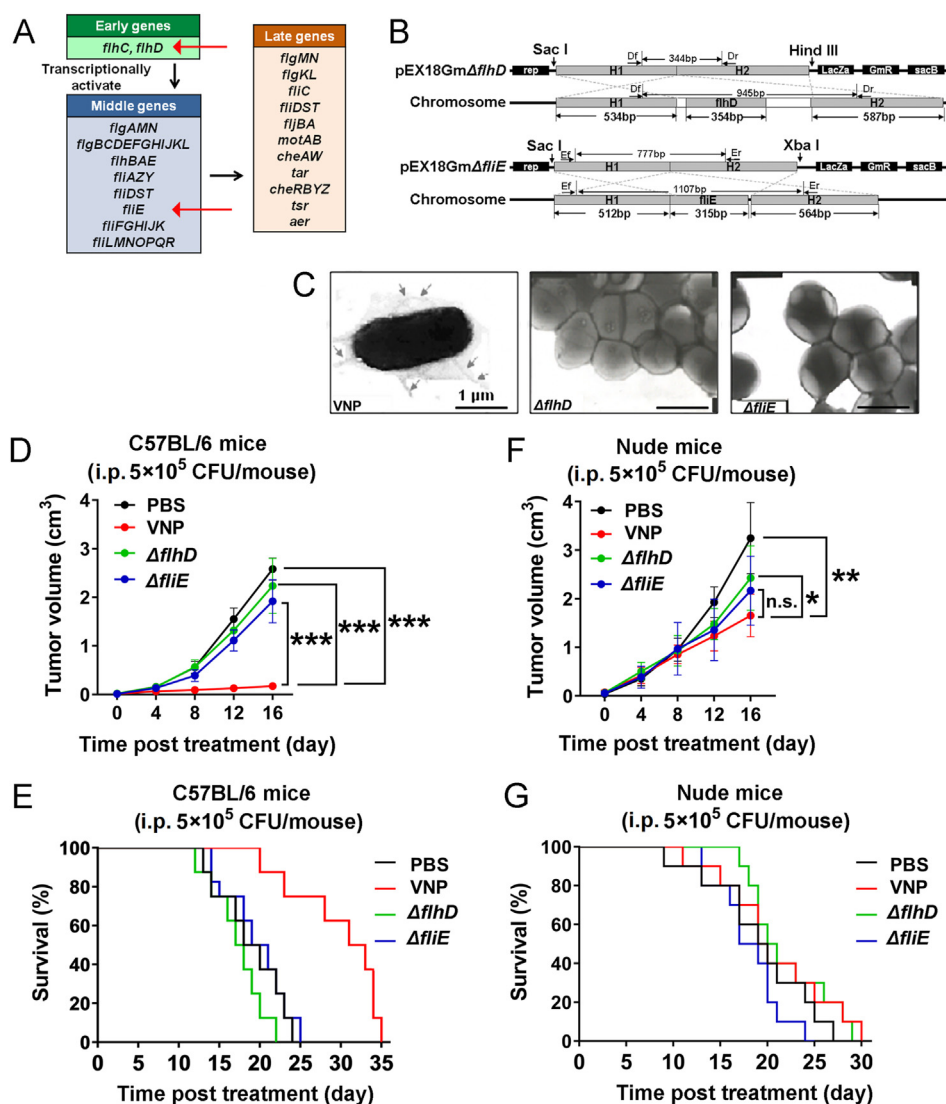


Figure 2 The disruption of flagella of VNP20009 significantly diminished its anti-tumor activity, especially in immunocompetent mice. (A) The critical genes regulating the production and assembling of flagella in *Salmonella*. Among these genes, Early genes are the master regulators which directly activate the expression of Middle genes and indirectly regulate Late genes. The temporal sequence of gene expression was shown by black arrows. The genes of interests were highlighted by red arrows. (B) The strategy for deleting *flhD* and *fljE* by double-crossover gene replacement. H1 and H2 represented homologous sequences. (C) The electron microscopic images showing the disruption of flagella in $\Delta flhD$ and $\Delta fljE$ strains. Immunocompetent (D) and immunodeficient (F) mice carrying melanoma allografts were intraperitoneally administered with phosphate-buffered saline (PBS) or an equal dose of wild-type VNP20009 (labelled as VNP in the figure), $\Delta flhD$ and $\Delta fljE$ strains. The tumor volumes were recorded and plotted as mean \pm SD, $n = 8$ for immunocompetent mice, $n = 10$ for immunodeficient mice. The Kaplan–Meier survival curves of immunocompetent (E) and immunodeficient (G) mice bearing melanoma allografts after intraperitoneal treatment of PBS or an equal dose of wild-type VNP20009, $\Delta flhD$ and $\Delta fljE$ strains. $n = 8$ for immunocompetent mice, $n = 10$ for immunodeficient mice. * $P < 0.05$; ** $P < 0.01$; *** $P < 0.001$; n.s. stands for nonsignificant. i.p. stands for intraperitoneally.

between the wild-type and $\Delta fljE$ strains (Fig. 3F and Fig. S3C), which could be further reduced to a nonsignificant difference if a higher dose of $\Delta fljE$ was used (Fig. 3G). By performing intratumoral injection of unequal doses of VNP20009 and $\Delta fljE$, their anti-tumor activity could be compared on the premise of equal infectivity. However, with equal initial intracellular colonization, the flagellum-deficient strain $\Delta fljE$ still exhibited significantly weakened anti-tumor activity (Fig. 3H). Moreover, intratumoral administration of heat-inactivated wild-type bacteria could still achieve a moderate suppressive effect on tumor growth in immunocompetent mice, which was still significantly weakened

if the flagellum-deficient strain $\Delta fljE$ was used (Fig. 3I). In this experiment, the dead wild-type bacteria had completely lost infectivity, but their anti-tumor activity partially remained.

These results suggest that the reduced infectivity does not fully explain why the destruction of flagella has such an adverse effect on the anti-tumor activity of VNP20009. Other mechanisms must contribute to this process parallelly. In addition to functioning as a locomotory organelle, the flagellum is also an important PAMP that strongly activates the host immune response³¹. Considering the emerging evidence showing how immune response can influence the development of cancer, we speculated that the flagellum-

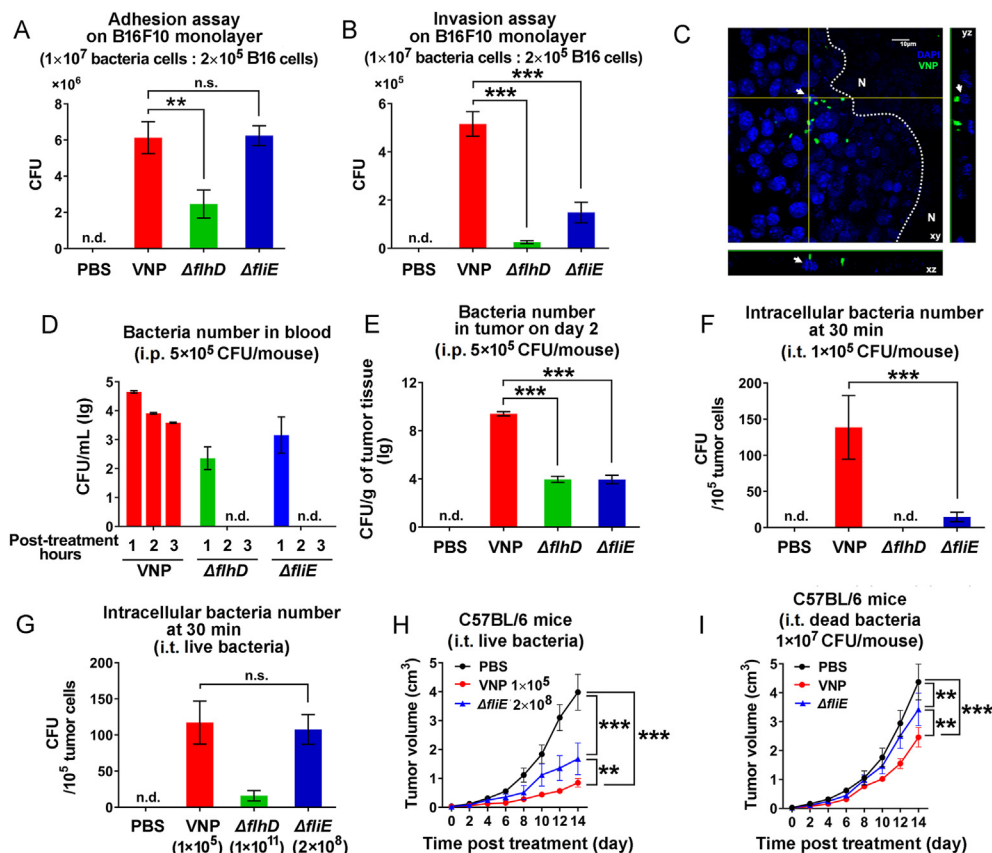


Figure 3 The flagellum-deficient strains exhibited reduced infectivity, which partially contributed to the loss of anti-tumor activity. The results of adhesion (A) and invasion (B) assays to compare the infectivity of wild-type VNP20009 (labelled as VNP in the figure), *ΔflhD* and *ΔfljE* strains on B16F10 monolayers *in vitro*. Data are mean ± SD, *n* = 3. (C) The representative fluorescent image of melanoma infected with eGFP-VNP20009. N, necrotic area. The bacterial titres in the peripheral blood (D) and tumors (E) after intraperitoneal treatment of wild-type VNP20009, *ΔflhD* and *ΔfljE* strains. Data are mean ± SD, *n* = 3. (F) The intracellular bacteria number was evaluated 30 min after the intratumoral treatment of an equal dose of wild-type VNP20009, *ΔflhD* and *ΔfljE* strains. Data are mean ± SD, *n* = 3. (G) The intracellular bacteria number was evaluated 30 min after the intratumoral treatment of various doses of wild-type VNP20009, *ΔflhD* and *ΔfljE* strains. Data are mean ± SD, *n* = 3. (H) The anti-tumor activity of wild-type VNP20009 and *ΔfljE* was evaluated by monitoring the tumor volume in the condition of an equal intracellular bacteria number by the intratumoral treatment of different doses of wild-type VNP20009 and *ΔfljE*. Data are mean ± SD, *n* = 8. (I) The infection-independent anti-tumor activity of wild-type VNP20009 and *ΔfljE* was evaluated by monitoring the tumor volume after the intratumoral treatment of heat-inactivated bacteria. Data are mean ± SD, *n* = 8. ***P* < 0.01; ****P* < 0.001; n.s. stands for nonsignificant. PBS: phosphate-buffered saline; i.p. stands for intraperitoneally; i.t. stands for intratumorally.

induced host immune response probably also plays an important role in the anti-tumor activity of *Salmonella*.

3.4. The activation of the host immune response was significantly weakened when flagellum-deficient bacteria were used

To test whether the flagellum-mediated host immune response has a role during VNP20009-mediated tumor therapy, both the systemic immune response and the intratumoral immune response were analysed after intraperitoneal administration of wild-type or flagellum-deficient strains in mice bearing melanoma allografts. Drastic enlargement of the spleen, which mainly contained highly activated T cells, was found only in mice that received wild-type VNP20009 (Fig. 4A–C and Fig. S4), suggesting that the destruction of flagella weakened the activation of the systemic immune response against *Salmonella* infection.

Similarly, significant increases in the levels of tumor-infiltrating CD4⁺ T cells (Fig. 4D), CD8⁺ T cells (Fig. 4E) and macrophages (Fig. 4F) were also observed only in mice that received wild-type bacteria. Consistently, a comprehensive analysis of the protein levels of cytokines showed that the flagellum-deficient strains induced much weaker inflammatory cytokine production in the tumor, than did the wild-type strains (Fig. 4G). T cells isolated from tumors treated with wild-type VNP20009 exhibited significantly higher RNA expression levels of key inflammatory cytokines including IL-4, IL-5, IL-13, IL-17, IL-21, IL-22 and IFN- γ , than did T cells extracted from tumors receiving flagellum-deficient strains (Fig. 4H). Indeed, Western blot analysis of the lysates of these tumor-infiltrating T cells showed higher phosphorylation levels for P65, P38, JNK and ERK, and a lower protein level of I κ B in the T cells extracted from tumors receiving wild-type VNP20009, indicating that two key downstream pathways of TLR signalling, the mitogen-activated protein kinase (MAPK) pathway and NF- κ B

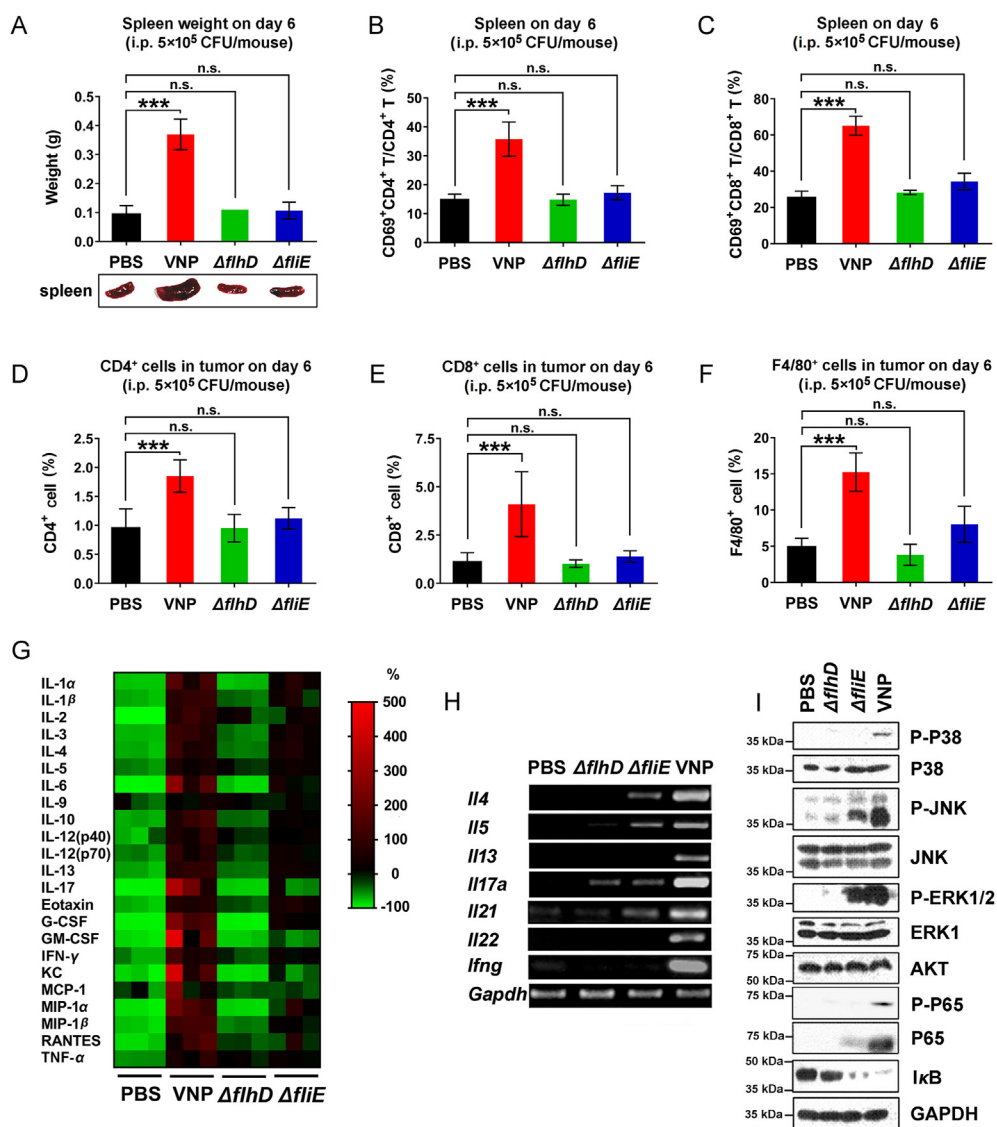


Figure 4 The activation of the host immune response was significantly weakened for the flagellum-deficient bacteria. (A) The weight of spleens of immunocompetent mice bearing melanoma allografts 6 days after the intraperitoneal treatment of wild-type VNP20009 (labelled as VNP in the figure), $\Delta flhD$ and $\Delta flhE$ strains. Data are mean \pm SD, $n = 3$. Representative images of resected spleens were shown below the columns. The percentage of CD69⁺ cells in total CD4⁺ T cells (B) and total CD8⁺ T cells (C) were measured by flow-cytometry 6 days after the intraperitoneal treatment of wild-type VNP20009, $\Delta flhD$ and $\Delta flhE$ strains. Data are mean \pm SD, $n = 3$. The percentage of CD4⁺ T cells (D), CD8⁺ T cells (E) and F4/80⁺ macrophages (F) infiltrating in tumors were measured by flow-cytometry 6 days after the intraperitoneally treatment of wild-type VNP20009, $\Delta flhD$ and $\Delta flhE$ strains. Data are mean \pm SD, $n = 3$. (G) The intratumoral concentrations of various inflammatory cytokines (C_a) were measured by Bio-Plex Multiplex Suspension Array 6 days after the intraperitoneal treatment of wild-type VNP20009, $\Delta flhD$ and $\Delta flhE$ strains. The fold change of the cytokine concentration (CC_a) relative to the mean of all mice (C_{mean}) was calculated by the formula: $CC_a = (C_a - C_{mean}) / C_{mean} \times 100\%$. The values were converted into colors and plotted. Green indicates reductions, and red indicates increase. (H) The RNA levels of *Il4*, *Il5*, *Il13*, *Il17a*, *Il21*, *Il22* and *Ifng* in the tumor-infiltrating T cells were compared by RT-PCR 6 days after the intraperitoneal treatment of wild-type VNP20009, $\Delta flhD$ and $\Delta flhE$ strains. (I) The activation status of ERK/JNK/MAPK and NF- κ B signaling pathways was evaluated by Western blots. *** $P < 0.001$; n.s. stands for nonsignificant. PBS: phosphate-buffered saline; i.p. stands for intraperitoneally.

pathway³², were strongly activated by only wild-type VNP20009 (Fig. 4I).

All these results suggest that the host immune response is specifically activated by the flagella of VNP20009, inducing the production of inflammatory factors, which may have a critical role in VNP20009-mediated cancer therapy.

3.5. Activation of the Flagellin/TLR5/NF- κ B pathway in the TME is crucial for the anti-tumor activity of VNP20009

Flagellin on the tip of flagella specifically binds and activates the receptor TLR5¹⁰, which is widely expressed on monocytes, macrophages, dendritic cells and CD4⁺ T cells. The binding

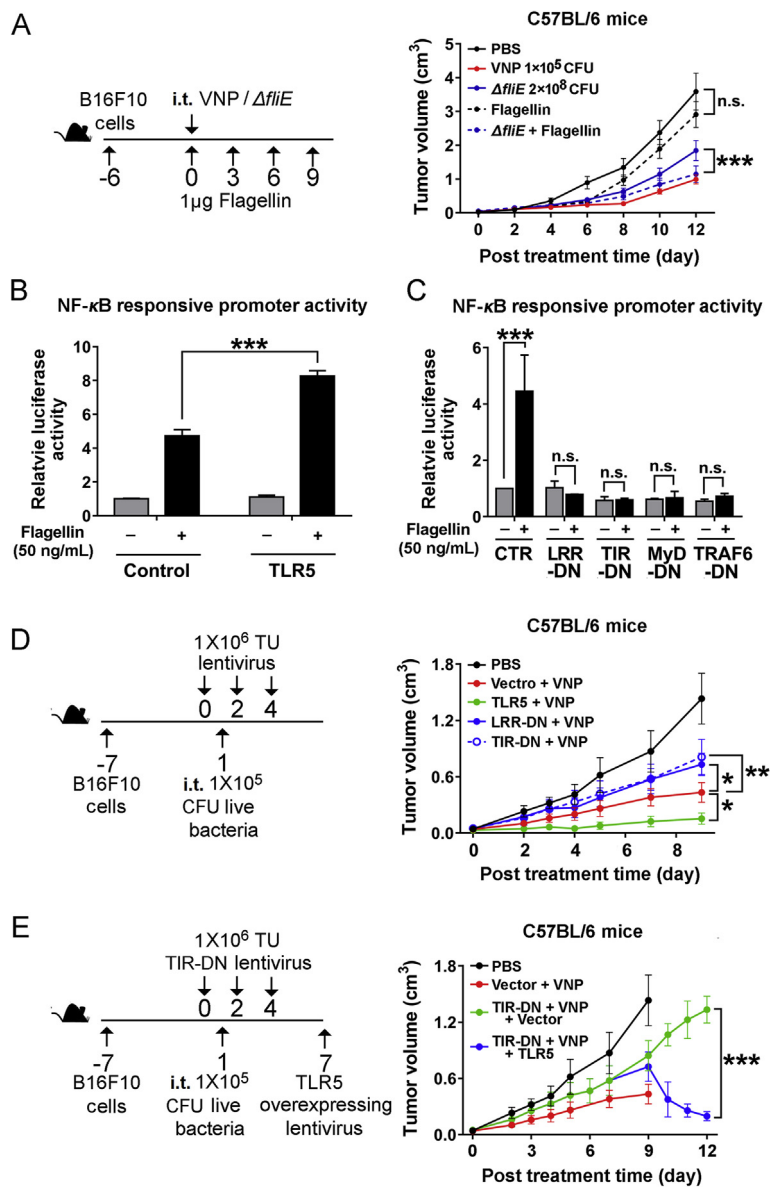


Figure 5 The activation of the Flagellin/TLR5/NF- κ B pathway in TME was crucial for the anti-tumor activity of VNP20009. (A) The immunocompetent mice were inoculated with melanoma allografts and intratumorally treated with wild-type VNP20009 (labelled as VNP in the figure) or a combination of wild-type VNP20009 and Δ *fljE*. The doses of bacteria were adjusted to achieve a similar intracellular bacteria number for wild-type VNP20009 and Δ *fljE* in the tumor. The treatment schedule was illustrated in the schematic diagram. The tumor volume was monitored and means \pm SD were plotted, $n = 8$. The activity of NF- κ B responsive promoter was evaluated in Jurkat cells after the treatment of Flagellin for 1 h. Jurkat cells were also transfected with either full-length TLR5 (B) or the dominant-negative (DN) truncates of TLR5 (LLR-DN, TIR-DN) and downstream transducers of TLR5-NF- κ B signaling pathway (MyD-DN, TRAF6-DN) (C). Data are mean \pm SD, $n = 3$. (D) The immunocompetent mice were inoculated with melanoma allografts and intratumorally treated with the combination of wild-type VNP20009 and lentivirus overexpressing full-length TLR5 or its dominant-negative truncates (LLR-DN, TIR-DN). The treatment schedule was illustrated in the schematic diagram. The tumor volume was monitored and the means \pm SD were plotted, $n = 8$. (E) The immunocompetent mice were inoculated with melanoma allografts and intratumorally treated with the combination of wild-type VNP20009 and lentivirus overexpressing dominant-negative truncates of TLR5 (TIR-DN). Seven days post the TIR-DN lentivirus treatment, lentivirus overexpressing full-length TLR5 were administered to rescue the effects of TIR-DN. The treatment schedule was illustrated in the schematic diagram. The tumor volume was monitored and the means \pm SD were plotted, $n = 8$. * $P < 0.05$; ** $P < 0.01$; *** $P < 0.001$; n.s. stands for nonsignificant. PBS: phosphate-buffered saline; i.p. stands for intraperitoneally; i.t. stands for intratumorally.

between Flagellin and TLR5 initiates the activation of TLR5/NF- κ B pathway and promotes the expression of various inflammatory cytokines. Theoretically, the combination of isolated Flagellin and

flagellum-deficient VNP20009 should restore the anti-tumor activity of flagellum-deficient strains if the host immune response truly has a crucial role in VNP20009-mediated cancer therapy. To

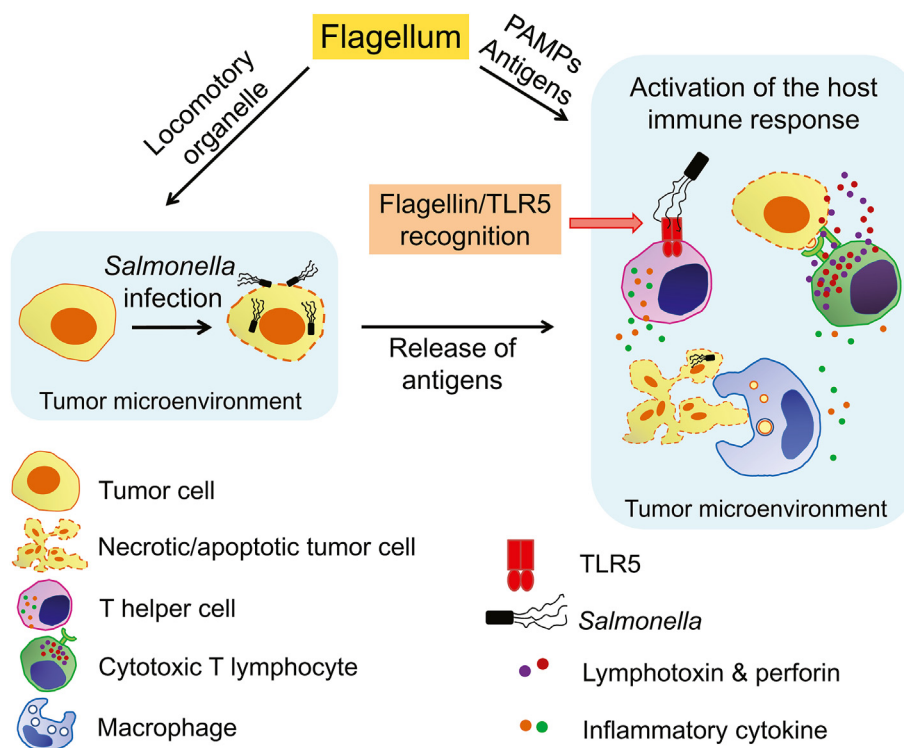


Figure 6 The schematic diagram illustrates the roles of flagella in *Salmonella*-mediated cancer therapy. Flagella are actively involved in *Salmonella*-mediated cancer therapy both as major locomotory organelles which increase the infectivity, as well as PAMPs activating the host immune response both systemically and intratumorally. The Flagellin/TLR5/NF- κ B signalling pathway plays an important role during this process.

test this hypothesis, wild-type VNP20009, the Δ *fljE* mutant or a combination of Flagellin and the Δ *fljE* mutant were administered i.t. to mice bearing melanoma. Flagellin alone exhibited a weak suppressive effect on tumor growth; while the combination of Flagellin and the Δ *fljE* mutant achieved remarkable anti-tumor activity that was comparable to the therapeutic effect of VNP20009, suggesting that the lack of Flagellin/TLR5/NF- κ B signalling could be an important factor causing the loss of anti-tumor activity foreseen with flagellum-deficient strains.

In Jurkat cells (an immortalized line of human T lymphocytes), overexpression of TLR5 enhanced the activation of the NF- κ B pathway upon Flagellin stimulation (Fig. 5B, Supporting Information Fig. S5A and S5B), which could be blocked by dominant-negative forms of TLR5, which consisted of either the extracellular domain with LRR motif or the intracellular TIR domain³³, as well as DN forms of MyD88 and TRAF6³⁴ (Fig. 5C and Fig. S5C). Overexpression of TLR5 or its DN forms showed little effect on the growth of B16F10 cells *in vitro* (Fig. S5D). However, intratumoral administration of TLR5 by a lentivirus could significantly enhance the anti-tumor activity of VNP20009, while the dominant-negative forms of TLR5 weakened the therapeutic effects of VNP20009 (Fig. 5D); this weakening could be rescued by reintroducing full-length TLR5 (Fig. 5E), indicating that the status of the Flagellin/TLR5/NF- κ B pathway in the TME, most likely in inflammatory cells, is critical for *Salmonella*-mediated cancer therapy.

Taken together, our study shows that flagella contribute to the anti-tumor activity of *Salmonella* both as locomotory organelles and as PAMPs activating the host immune response in the TME (Fig. 6). Decreasing the infectivity and immunogenicity of

Salmonella by destroying flagella impairs its anti-tumor activity, while enhancing the host immune response by activating the Flagellin/TLR5/NF- κ B pathway can improve the efficacy of *Salmonella*-mediated cancer therapy.

4. Discussion

Our study showed that the flagellum of *Salmonella* is critical for the activation of the host immune response, turning the immunosuppressive TME into an immune-active TME during *Salmonella*-mediated cancer therapy. Recently, Min et al.³⁵ reported that engineered *Salmonella typhimurium* inducibly secreting *Vibrio vulnificus* Flagellin B could promote M1-like macrophage polarization in the TME to strongly suppress the growth of tumors in a host TLR signalling pathway-dependent manner. Our observation reconfirmed the importance of flagella in *Salmonella*-mediated cancer therapy in an independent experimental setting.

There are still debates about whether bacteria must enter tumor cells before killing them. Moreover, it is not clear whether VNP20009 enters tumor cells *via* active infection or passive endocytosis. Even though we measured the intracellular bacteria number with a gentamicin protection assay in this study, it is worth noting that this method might lead to an incorrect conclusion, since bacteria temporarily surviving within phagosomes would contaminate the final count of live bacteria colonizing tumor cells. This study mainly focused on the immunogenic role of Flagellin during *Salmonella*-mediated cancer therapy, and these effects could be achieved in the absence of intracellular bacteria. More experiments precisely analysing the processes and consequences of bacteria entering tumor cells should be conducted to

establish a solid causal relationship between bacteria entering tumor cells and the death of tumor cells.

In addition to the activation of the TLR signalling pathway by LPS and Flagellin, cancer-specific antigens also contribute to *Salmonella*-mediated cancer therapy. The drastic tumor cell lysis caused by *Salmonella* infection provides a substantial pool of antigens for antigen-presenting cells, potentiating the generation of tumor-specific cytotoxic T cells and memory T cells and leading to long-term protection against metastasis and recurrence³⁶, similar to the effects of cancer vaccination or adoptive T cell therapy. However, the response rate of peptide-based cancer vaccination is generally unsatisfactory probably due to the heterogeneity of cancer³⁷, while personalized adoptive T cell therapy sometimes leads to a lethal autoimmune response due to the similarities between cancer cells and healthy cells. For example, transferring T cells targeting ERB-B2 receptor tyrosine kinase 2 (ERBB2), a cell-surface protein overexpressed by various kinds of cancer, can cause serious adverse effects due to T cells mistakenly attacking the lung epithelium, which exhibits a low level of ERBB2 expression³⁸. The limitation of stringently cancer-specific antigens and the possibility for engineered T cells to cross-react to an endogenous antigen with a similar structure hamper the safety of such therapies for general applications³⁹. In contrast, *Salmonella*-mediated cancer therapies utilize autologous T cells that have undergone thymic selection, preventing severe systemic autoimmune reactions.

Cancer immunotherapies based on immune checkpoint inhibitors are also developing rapidly. Monoclonal antibodies against PD-1/PD-L1 (pembrolizumab and nivolumab) and cytotoxic T-lymphocyte-associated protein 4 (CTLA-4) (ipilimumab) have been approved for the treatment of Hodgkin lymphoma⁴⁰ and melanoma^{41,42}, but their effects are hampered in tumors with a low level of T cell infiltration⁴³. Therefore, *Salmonella*-mediated cancer therapy holds promise for improving the efficacy of immune checkpoint inhibitors in such circumstances by actively attracting more lymphocytes into the hypoxic centre of tumors, which *Salmonella* preferentially colonizes. Combinations of *Salmonella* with PD-1 antibody, CTLA-4 antibody and adoptive T cell therapy have been evaluated in tumor-bearing mice, which achieved encouraging improvement in tumor burden reduction and relapse prevention^{44,45}.

To date, many compounds of different chemical constitutions have been designed for the specific activation of TLRs, such as, polyAU for TLR3⁴⁶, and synthetic small-molecule compounds targeting TLR7/8⁴⁷. However, since the expression of TLRs is not strictly restricted to immune cells⁴⁸, more investigations must be conducted to evaluate the biological effects of these compounds on antigen presenting cells, lymphocytes and tumor cells to obtain practical guidance for the safe application of TLR agonists in cancer immunotherapy.

5. Conclusions

Our findings regarding the importance of the Flagellin/TLR5/NF- κ B pathway in *Salmonella*-mediated cancer therapy suggest that agonists of TLRs can also be used in cancer immunotherapies.

Acknowledgments

This study was supported by grants from the Jiangsu Provincial Nature Science Foundation (BK20192005, China), National

Natural Science Foundation of China (81630092, 81903143, 81802338, and 82072646), Zhejiang Provincial Natural Science Foundation of China for Distinguished Young Scholars (LR21H160001) and Start-up Grant of HZNU (4125C5021820470, China). We thank Dr. Wenhui Jiang for her assistance for the immunohistochemical staining during the experiments and thank Dr. Dongping Wei for his encouragement on the setup of this project. We are grateful to the mice for their contributions to this study.

Author contributions

Zichun Hua and Jianxiang Chen designed experiment. Jianxiang Chen and Yiting Qiao performed most assays and wrote the manuscript. Guo Chen, Cunjie Chang and Heng Dong contributed to the genetic modifications of bacteria and *in vitro* experiments. Bo Tang, Xiawei Cheng and Xiufeng Liu helped with animal experiments.

Conflicts of interest

The authors have no conflicts of interest to declare.

Appendix A. Supporting information

Supporting data to this article can be found online at <https://doi.org/10.1016/j.apsb.2021.04.019>.

References

- Forbes NS. Engineering the perfect (bacterial) cancer therapy. *Nat Rev Cancer* 2010;**10**:785–94.
- Pawelek JM, Low KB, Bermudes D. Tumor-targeted *Salmonella* as a novel anticancer vector. *Cancer Res* 1997;**57**:4537–44.
- Kohwi Y, Imai K, Tamura Z, Hashimoto Y. Antitumor effect of Bifidobacterium infantis in mice. *Gan* 1978;**69**:613–8.
- Yu YA, Shabahang S, Timiryasova TM, Zhang Q, Beltz R, Gentshev I, et al. Visualization of tumors and metastases in live animals with bacteria and vaccinia virus encoding light-emitting proteins. *Nat Biotechnol* 2004;**22**:313–20.
- Parker RC, Plummer HC. Effect of histolyticus infection and toxin on transplantable mouse tumors. *Proc Soc Exp Biol Med* 1947;**66**:461–7.
- Malmgren RA, Flanigan CC. Localization of the vegetative form of *Clostridium tetani* in mouse tumors following intravenous spore administration. *Cancer Res* 1955;**15**:473–8.
- Mroczenski-Wildey MJ, Di Fabio JL, Cabello FC. Invasion and lysis of HeLa cell monolayers by *Salmonella typhi*: the role of lipopolysaccharide. *Microb Pathog* 1989;**6**:143–52.
- Stern C, Kasnitz N, Kocijancic D, Trittel S, Riese P, Guzman CA, et al. Induction of CD4⁺ and CD8⁺ anti-tumor effector T cell responses by bacteria mediated tumor therapy. *Int J Cancer* 2015;**137**:2019–28.
- Mittrucker HW, Kaufmann SH. Immune response to infection with *Salmonella typhimurium* in mice. *J Leukoc Biol* 2000;**67**:457–63.
- Hayashi F, Smith KD, Ozinsky A, Hawn TR, Yi EC, Goodlett DR, et al. The innate immune response to bacterial flagellin is mediated by Toll-like receptor 5. *Nature* 2001;**410**:1099–103.
- Wright SD, Ramos RA, Tobias PS, Ulevitch RJ, Mathison JC. CD14, a receptor for complexes of lipopolysaccharide (LPS) and LPS binding protein. *Science* 1990;**249**:1431–3.
- Shimazu R, Akashi S, Ogata H, Nagai Y, Fukudome K, Miyake K, et al. MD-2, a molecule that confers lipopolysaccharide responsiveness on Toll-like receptor 4. *J Exp Med* 1999;**189**:1777–82.

13. Mantovani A, Allavena P, Sica A, Balkwill F. Cancer-related inflammation. *Nature* 2008;**454**:436–44.
14. Smyth MJ, Hayakawa Y, Takeda K, Yagita H. New aspects of natural-killer-cell surveillance and therapy of cancer. *Nat Rev Cancer* 2002;**2**: 850–61.
15. Rubio V, Stuge TB, Singh N, Betts MR, Weber JS, Roederer M, et al. *Ex vivo* identification, isolation and analysis of tumor-cytolytic T cells. *Nat Med* 2003;**9**:1377–82.
16. Hung K, Hayashi R, Lafond-Walker A, Lowenstein C, Pardoll D, Levitsky H. The central role of CD4⁺ T cells in the antitumor immune response. *J Exp Med* 1998;**188**:2357–68.
17. Mumberg D, Monach PA, Wanderling S, Philip M, Toledano AY, Schreiber RD, et al. CD4⁺ T cells eliminate MHC class II-negative cancer cells *in vivo* by indirect effects of IFN-gamma. *Proc Natl Acad Sci U S A* 1999;**96**:8633–8.
18. Boon T, Coulie PG, Van den Eynde BJ, van der Bruggen P. Human T cell responses against melanoma. *Annu Rev Immunol* 2006;**24**:175–208.
19. Gajewski TF, Meng Y, Harlin H. Immune suppression in the tumor microenvironment. *J Immunother* 2006;**29**:233–40.
20. Liu Y, Liu X, Zhang N, Yin M, Dong J, Zeng Q, et al. Berberine diminishes cancer cell PD-L1 expression and facilitates antitumor immunity *via* inhibiting the deubiquitination activity of CSN5. *Acta Pharm Sin B* 2020;**10**:2299–312.
21. Wang Z, Kang W, Li O, Qi F, Wang J, You Y, et al. Abrogation of USP7 is an alternative strategy to downregulate PD-L1 and sensitize gastric cancer cells to T cells killing. *Acta Pharm Sin B* 2021;**11**:694–707.
22. Topalian SL, Hodi FS, Brahmer JR, Gettinger SN, Smith DC, McDermott DF, et al. Safety, activity, and immune correlates of anti-PD-1 antibody in cancer. *N Engl J Med* 2012;**366**:2443–54.
23. Low KB, Ittensohn M, Luo X, Zheng LM, King I, Pawelek JM, et al. Construction of VNP20009: a novel, genetically stable antibiotic-sensitive strain of tumor-targeting *Salmonella* for parenteral administration in humans. *Methods Mol Med* 2004;**90**:47–60.
24. Toso JF, Gill VJ, Hwu P, Marincola FM, Restifo NP, Schwartzentruber DJ, et al. Phase I study of the intravenous administration of attenuated *Salmonella typhimurium* to patients with metastatic melanoma. *J Clin Oncol* 2002;**20**:142–52.
25. Chen J, Qiao Y, Tang B, Chen G, Liu X, Yang B, et al. Modulation of *Salmonella* tumor-colonization and intratumoral anti-angiogenesis by triptolide and its mechanism. *Theranostics* 2017;**7**:2250–60.
26. Fan Y, Evans CR, Ling J. Reduced protein synthesis fidelity inhibits flagellar biosynthesis and motility. *Sci Rep* 2016;**6**:30960.
27. Winkelstroter LK, De Martinis EC. *In vitro* protective effect of lactic acid bacteria on *Listeria monocytogenes* adhesion and invasion of Caco-2 cells. *Benef Microbes* 2015;**6**:535–42.
28. Qiao Y, Chen J, Lim YB, Finch-Edmondson ML, Seshachalam VP, Qin L, et al. YAP regulates actin dynamics through ARHGAP29 and promotes metastasis. *Cell Rep* 2017;**19**:1495–502.
29. Chang LJ, Zais AK. Self-inactivating lentiviral vectors and a sensitive Cre-loxP reporter system. *Methods Mol Med* 2003;**76**:367–82.
30. Chevance FF, Hughes KT. Coupling of flagellar gene expression with assembly in *Salmonella enterica*. *Methods Mol Biol* 2017;**1593**: 47–71.
31. Feuillet V, Medjane S, Mondor I, Demaria O, Pagni PP, Galan JE, et al. Involvement of Toll-like receptor 5 in the recognition of flagellated bacteria. *Proc Natl Acad Sci U S A* 2006;**103**:12487–92.
32. Takeda K, Akira S. TLR signaling pathways. *Semin Immunol* 2004;**16**: 3–9.
33. Ivison SM, Khan MA, Graham NR, Bernales CQ, Kaleem A, Tirling CO, et al. A phosphorylation site in the Toll-like receptor 5 TIR domain is required for inflammatory signalling in response to flagellin. *Biochem Biophys Res Commun* 2007;**352**:936–41.
34. Burns K, Martinon F, Esslinger C, Pahl H, Schneider P, Bodmer JL, et al. MyD88, an adapter protein involved in interleukin-1 signaling. *J Biol Chem* 1998;**273**:12203–9.
35. Zheng JH, Nguyen VH, Jiang SN, Park SH, Tan W, Hong SH, et al. Two-step enhanced cancer immunotherapy with engineered *Salmonella typhimurium* secreting heterologous flagellin. *Sci Transl Med* 2017;**9**:eaak9537.
36. Avogadri F, Martinoli C, Petrovska L, Chiodoni C, Transidico P, Bronte V, et al. Cancer immunotherapy based on killing of *Salmonella*-infected tumor cells. *Cancer Res* 2005;**65**:3920–7.
37. Rosenberg SA, Yang JC, Restifo NP. Cancer immunotherapy: moving beyond current vaccines. *Nat Med* 2004;**10**:909–15.
38. Morgan RA, Yang JC, Kitano M, Dudley ME, Laurecot CM, Rosenberg SA. Case report of a serious adverse event following the administration of T cells transduced with a chimeric antigen receptor recognizing ERBB2. *Mol Ther* 2010;**18**:843–51.
39. Caspi RR. Immunotherapy of autoimmunity and cancer: the penalty for success. *Nat Rev Immunol* 2008;**8**:970–6.
40. Kasamon YL, de Claro RA, Wang Y, Shen YL, Farrell AT, Pazdur R. FDA approval summary: nivolumab for the treatment of relapsed or progressive classical Hodgkin lymphoma. *Oncol* 2017;**22**:585–91.
41. Barone A, Hazarika M, Theoret MR, Mishra-Kalyani P, Chen H, He K, et al. FDA approval summary: pembrolizumab for the treatment of patients with unresectable or metastatic melanoma. *Clin Cancer Res* 2017;**23**:5661–5.
42. Camacho LH. CTLA-4 blockade with ipilimumab: biology, safety, efficacy, and future considerations. *Cancer Med* 2015;**4**:661–72.
43. Tang H, Wang Y, Chlewicki LK, Zhang Y, Guo J, Liang W, et al. Facilitating T cell infiltration in tumor microenvironment overcomes resistance to PD-L1 blockade. *Cancer Cell* 2016;**29**:285–96.
44. Ebelt ND, Zuniga E, Marzagalli M, Zamloot V, Blazar BR, Salgia R, et al. *Salmonella*-based therapy targeting indoleamine 2,3-dioxygenase restructures the immune contexture to improve checkpoint blockade efficacy. *Biomedicines* 2020;**8**:617.
45. Binder DC, Arina A, Wen F, Tu T, Zhao M, Hoffman RM, et al. Tumor relapse prevented by combining adoptive T cell therapy with *Salmonella typhimurium*. *Oncol Immunology* 2016;**5**:e1130207.
46. Cheng YS, Xu F. Anticancer function of polyinosinic-polycytidylic acid. *Cancer Biol Ther* 2010;**10**:1219–23.
47. Weeratna RD, Makinen SR, McCluskie MJ, Davis HL. TLR agonists as vaccine adjuvants: comparison of CpG ODN and Resiquimod (R-848). *Vaccine* 2005;**23**:5263–70.
48. So EY, Ouchi T. The application of Toll like receptors for cancer therapy. *Int J Biol Sci* 2010;**6**:675–81.